8094 *Macromolecules* **2010**, *43*, 8094–8100
DOI: 10.1021/ma101639w

Macromolecules
ARTICLE

Functional Polymeric Nanoobjects by Cross-Linking Bulk Self-Assemblies of Poly(*tert*-butyl acrylate)-*block*-poly(glycidyl methacrylate)

Jianglei Qin, Xiubo Jiang, Lei Gao, Yongming Chen,* and Fu Xi

Laboratory of Polymer Physics and Chemistry, Institute of Chemistry, The Chinese Academy of Sciences, Beijing 100190, China

Received July 21, 2010; Revised Manuscript Received August 25, 2010

ABSTRACT: We report the bulk self-assembly of diblock copolymer poly(*tert*-butyl acrylate)-*block*-poly(glycidyl methacrylate) (P*t*BA-*b*-PGMA) with the PGMA that bears many epoxy groups as a cross-linkable segment and the P*t*BA as a hydrolyzable segment. The P*t*BA-*b*-PGMA block copolymers of a different composition were synthesized by two-step atom transfer radical polymerization (ATRP). After bulk self-assembly, the morphologies of microphase separation of the block copolymers were studied with small-angle X-ray scattering (SAXS) and transmission electron microscopy (TEM). The results showed that with decrease of volume ratio of the PGMA segments the P*t*BA-*b*-PGMA self-assembled into lamellae, cylinders, and spheres with the dispersed PGMA domains. The epoxy groups in the PGMA domains were cross-linked by exposing the microphase-separated films into an atmosphere of either ethylenediamine (EDA) or propargylamine (PA). Then the bulk materials were dispersed into the good solvent of P*t*BA to generate the polymeric nanoobjects of plates, fibers, and spheres, of which the cross-linked PGMAs were the cores and the P*t*BAs were the coronas. After hydrolysis of the P*t*BA segments into the poly(acrylic acid)s (PAAs), the cross-linked nanoobjects could be dispersed in basic water and showed reversible pH responsibility. The pendant alkyne groups in the PA cross-linked nanoobjects were applied to anchor anthracenes by click reaction with 9-(azidomethyl)anthracene (9-AMA).

Introduction

Block copolymers can self-assemble spontaneously into various ordered nanostructures in bulk. Depending on the parameters of the constituents, such as volume fractions and interaction of different blocks, ordered lamellar, cylindrical, and spherical morphologies are commonly found.[1] These ordered structures have a great potential application in nanomaterials and nanotechnologies related to patterning, loading, optics, catalysis, etc.[2,3] Therefore, the microphase separation of block copolymers and functional nanomaterials thereof have attracted much interest in recent years.[4−11] Furthermore, by cross-linking the discontinuous domains of the preformed self-assemblies of the block copolymers and dispersing them in a good solvent of the un-cross-linked domains, a range of nanoobjects with controlled shape and size are easily obtained. To prepare bulk self-assemblies with the cross-linkable domains, a series of block copolymers with cross-linkable blocks, such as the copolymers with poly(2-cinnamoyloxyethyl methacrylate) (PCEMA), polybutadiene (PB), poly(3-(triethoxysilyl)propyl methacrylate) (PTEPM), and polyisoprene segments, have been investigated intensively.[12−23] Liu et al. have used the triblock copolymers of PCEMA to prepare isolated nanotubes, where Fe_2O_3 or Pd nanoparticles were impregnated inside the nanocavities.[12−14] Müller et al. have applied the PB block copolymers to prepare the core cross-linked Janus micelles, disks, cylinders, and other nanoobjects.[15−18] This group has reported a series of microphase-separated block copolymers of PTEPM whose microdomains can be cross-linked by gelating reaction of triethoxysilyl groups, and then organic/inorganic hybrid nanoobjects of different shape were prepared.[19−23] Moreover, the dispersed nanoobjects with poly(2-vinylpyridine) hairs had been applied to load a large amount of Au nanoparticles.[21,22] These block copolymer self-assemblies can be cross-linked with appropriate methods, and the shaped polymeric nanoobjects may be generated easily. In order to explore their application, it is necessary to introduce functional groups either into the cross-linked cores or the corona of these copolymeric nanoobjects.

Glycidyl methacrylate is a functional monomer with both vinyl group and epoxy group in its molecular structure and can be polymerized by both radical polymerization and ring-opening polymerization.[24,25] The radical polymerized poly(glycidyl methacrylate) (PGMA) bears pendant epoxy groups that are readily to be cross-linked with a variety of amines. At the same time, the amines to react with epoxy can bear various functional groups; therefore, they not only can act as cross-linking agents but also may endow the cross-linked domains with variety of functionalities. Although cross-linking of PGMA copolymers in solution have been studied,[26,27] the bulk self-assembly of PGMA block copolymers has not been reported yet.

As our continuous effort to fabricate the shaped polymeric nanoobjects using functional block copolymers,[19−23] herein we report the reactive self-assemblies prepared from P*t*BA-*b*-PGMA with PGMA as a cross-linkable segment in bulk. The P*t*BA as another segment of block copolymers was selected because it can be hydrolyzed into the PAA segments to show pH responsibility and other functions. Although the PAA block copolymers have been studied intensively,[12−14,28−30] water-dispersible block copolymer nanoobjects stabilized with the tethered PAA hairs in different morphologies were seldom reported.[16] The P*t*BA-*b*-PGMA was synthesized with a two-step ATRP procedure. As shown in Scheme 1, the block copolymers of different composition self-assembled into lamellae, cylinders, and spheres in bulk. After cross-linking of PGMA domains under an atmosphere of amines, the materials with ordered nanostructures were dispersed

---

*Corresponding author. E-mail: ymchen@iccas.ac.cn.

Scheme 1. Preparation of Functional Nanoobjects with Different Morphologies by the Procedure of Microphase-Separated P*t*BA-*b*-PGMA Block Copolymers, Cross-Linking PGMA Domains, and Dispersing in Solvent of P*t*BA[a]

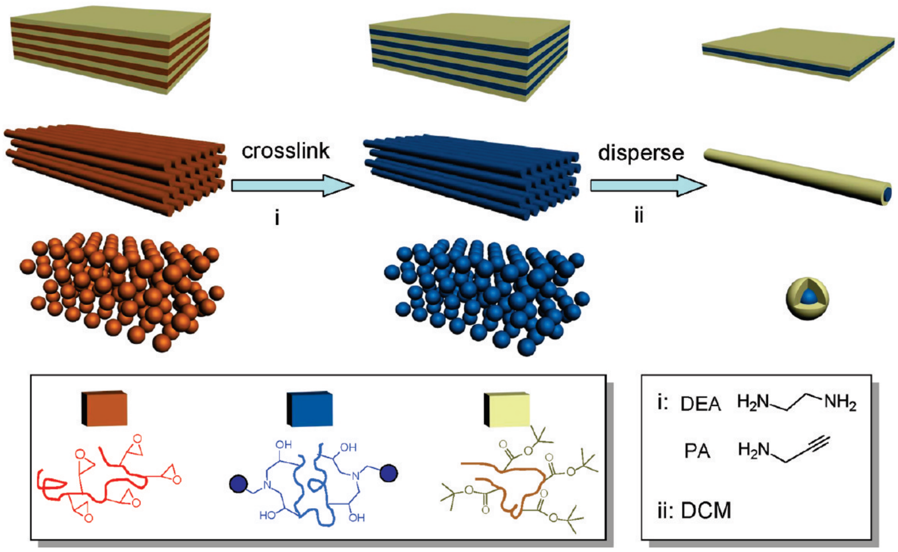

[a] The P*t*BA domains in cylindrical and spherical phases were not shown.

in solvents to form well-defined nanoobjects of different morphologies. Furthermore, the P*t*BA segments were hydrolyzed into the PAAs, and the dispersed nanoobjects were extracted into water to give water-dispersible nanoobjects with pH responsibility. The water-dispersed nanoobjects have potential applications owing to that the PAAs can be applied to load nanoparticles[12-14] or induce macroscopically ordered polymer/$CaCO_3$ hybrids.[31] Another interesting thing is that, besides inducing cross-links in the PGMA domains, additive primary amines bearing functional groups can endow the nanoobjects with more functionalities. Herein when propargylamine (PA) was used to cross-link the PGMA domains, the alkyne groups were introduced into the nanoobjects at the same time, and they were applied to conduct click chemistry of cycloaddition with the azide groups.[32,33] Also, the azide groups could be introduced into the partial cross-linked nanoobjects by reaction between the remained epoxy groups and NaN_3.

Experimental Section

Materials. Glycidyl methacrylate (GMA, Aldrich) and *tert*-butyl acrylate (*t*BA, Alfa Aesar) were purified by vacuum distillation prior to use. 9-(Azidomethyl)anthracene (9-AMA) was synthesized and purified according to literature.[34] Ethyl 2-bromoisobutyrate (EBiB) (Aldrich), *N*,*N*,*N*′,*N*″,*N*″-pentamethyldiethylenetriamine (PMDETA) (Aldrich), PA (Bainaite), EDA, CF_3COOH (TFA), and other chemicals were used as received.

Homopolymerization of *t*BA. A typical procedure to prepare the bromine end-functionalized P*t*BA is as follows. EBiB (39 mg, 0.2 mmol), PMDETA (42 μL, 0.2 mmol), *t*BA (5.12 g, 40 mmol), and acetone (1.5 mL) were added into a 20 mL flask. The mixture was degassed by three freeze−evacuate−thaw cycles, and then the CuBr (28.8 mg, 0.2 mmol) was added into the flask. The flask was sealed under vacuum after evacuated and backfilled with nitrogen twice. The polymerization was carried out in an oil bath at 60 °C for 6 h. The resulted crude product was passed through a column filled with neutral alumina and purified by precipitating into a large amount of methanol and water mixture (1:1 volume ratio) three times. The molar mass, M_n = 11 000, was evaluated by monomer conversion, and the polydispersity index, PDI = 1.08, was determined by size exclusive chromatography (SEC) with standard PS calibration.

Diblock Copolymerization. The bromine end-functionalized P*t*BA was applied as the macroinitiator to synthesize P*t*BA-*b*-PGMA with halogen exchange since the GMA polymerization can be well mediated with CuCl/PMDETA as catalyst.[24,35] P*t*BA-Br (330 mg, 0.03 mmol), PMDETA (6.3 μL, 0.03 mmol), GMA (0.43 g, 3 mmol), and acetone (1 mL) were added into a 10 mL flask. The CuCl (3 mg, 0.03 mmol) was added into the flask after degassed by three freeze−evacuate−thaw cycles. Then the flask was sealed, evacuated, and backfilled with nitrogen twice, and the polymerization was carried out under nitrogen in an oil bath at 50 °C. The product was purified by precipitating into a large amount of methanol and water mixture (2:1 volume ratio), and the block ratio of the copolymers was determined by the ^{1}H NMR spectra with $CDCl_3$ as solvent.

Bulk Self-Assembly of P*t*BA-*b*-PGMA Block Copolymers. The solution of P*t*BA-*b*-PGMA diblock copolymer (50 mg/mL) in CH_2Cl_2 (DCM) was spread onto a clean Teflon plate, and the solvent was allowed to evaporate slowly in a DCM atmosphere in a vacuum desiccator. The resulting bulk films (ca. 0.5 mm in thickness) were then dried for 12 h under vacuum at 40 °C. Thermal annealing was conducted at 80 °C for 24 h under argon to give the materials with microphase separation due to the T_g of PGMA is 74 °C[36] and the T_g of P*t*BA is around 40 °C.[37]

Cross-Linking of PGMA Domains and Preparation of Nanoobjects. An atmosphere of the amines was generated by dropping EDA or PA in a closed container. The P*t*BA-*b*-PGMA bulk materials were exposed to the atmospheres of amines at room temperature for a period of time, and the unreacted amines were removed under vacuum. After cross-linking, the samples were immersed into DCM with 1 mg/mL and stirred vigorously. The TEM investigations were performed after the samples were dispersed into homogeneous dispersions. The hydrolysis of the P*t*BA segments of nanoobjects was carried out in DCM dispersions for 24 h with an excess of TFA as catalyst; then the nanoobjects were extracted with 1 M of KOH aqueous solution. The TEM investigations were performed after the dispersions were dialyzed against water until pH = 7.

Click Reactions on PA Cross-Linked Nanofibers. 10 mg of the PA cross-linked P*t*BA$_{86}$-*b*-PGMA$_{40}$ fibers was dispersed in 5 mL of DMF, and then 7.0 mg (0.03 mmol) of 9-AMA and 6.4 μL (0.03 mmol) of PMDETA were added into the dispersion. 4.3 mg of CuBr (0.03 mmol) was added in solid state after the dispersion was degassed by three freeze−pump−thaw cycles. After reacted for 24 h under nitrogen at 60 °C, the nanoobjects were precipitated and dried under vacuum. To remove the unreacted 9-AMA completely, the nanoobjects were hydrolyzed by CF_3COOH and extracted into 1 M KOH aqueous solution after

Scheme 2. Synthesis of P*t*BA and Its Block Copolymer of PGMA by Two-Step ATRP

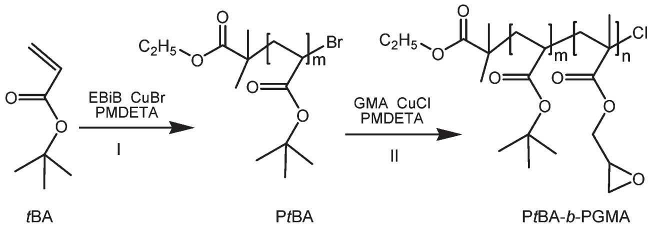

washed three times with DCM. The UV characterization was performed after the water dispersion was dialyzed until pH = 7.

Postmodification of EDA Cross-Linked Nanoplates. The remained epoxy groups of the EDA cross-linked nanoplates were further modified in DMF dispersion as follows. 40 mg of the EDA cross-linked P*t*BA$_{100}$-*b*-PGMA$_{95}$ nanoplates (its characteristic and characterization are given in the Supporting Information) was dispersed in 5 mL of DMF, and then 100 mg of NaN_3 and 125 mg of NH_4Cl were dissolved in the mixture and stirred overnight. After being purified and dried in vacuum, the nanoplates were dispersed in DCM and then casted on a KBr plate for Fourier-transform infrared (FT-IR) characterization.

Characterizations. SEC was performed on a Waters 515 HPLC pump equipped with a set of Waters Styragel columns and a Waters 2414 refractive index detector. THF was used as eluent at a flow rate of 1.0 mL/min with PS calibration. ^{1}H NMR spectra were recorded on a Bruker AV400 spectrometer with $CDCl_3$ as solvent at room temperature. FT-IR spectra were recorded on Thermo Nicolet Avatar-330 spectrometer, and the samples were prepared by solvent casting on a KBr plate. UV spectra were recorded on a TU-1901 spectrometer in water dispersions. Transmission electron microscopy (TEM) images were obtained on a Hitachi H-800 instrument operated at an accelerating voltage of 100 kV, and the images were recorded by a digital camera. Bulk samples were embedded in epoxy resin and cured at room temperature overnight. Thin slices (50−100 nm) were obtained using an ultramicrotome with a diamond knife at room temperature. The microtomed slices were stained by RuO_4 vapor for 2 h before observation. Dispersed samples were dropped onto carbon-coated grids for TEM observation. SAXS experiments were performed on an incorporate SAXS system; the wavelength of the incident X-ray beam from Cu Kα radiation is $\lambda = 0.154$ nm.

Results and Discussion

Synthesis and Characterization of P*t*BA-*b*-PGMA Diblock Copolymers. P*t*BA-*b*-PGMA diblock copolymers were synthesized by a two-step ATRP procedure (Scheme 2), in which the first P*t*BA block was polymerized with EBiB as the initiator and CuBr/PMDETA as the catalyst at 60 °C, and the degree of polymerization (DP) was evaluated by monomer conversion. Since the halogen exchange between the bromide end of the P*t*BA and the catalyst was necessary to give a high efficiency of the chain extension from the P*t*BA to the PGMA, CuCl/PMDETA was applied in the second step of ATRP of GMA and the SEC traces showed that the P*t*BA initiated the PGMA successfully. Three diblock copolymers with different block composition were synthesized, and their characteristics are listed in Table 1. Their SEC traces were collected in Figure S1 (in Supporting Information). As an example, the ^{1}H NMR spectrum of P*t*BA$_{86}$-*b*-PGMA$_{40}$ block copolymer with 34.1% weight fraction of PGMA is shown in Figure S2 (in Supporting Information). The block ratio was calculated by comparing the peak areas of the protons derived from two blocks, for example, the peak b (H in the epoxy ring) in PGMA block and the peak d (H adjacent to carbonyl group) in P*t*BA block.

Table 1. Characteristics of P*t*BA-*b*-PGMA Block Copolymers and Microphase Separation

sample	$M_n \times 10^{-4}$	wt % PGMA[a]	PDI[b]	morphology	*d*-spacing[c] (nm)
P*t*BA$_{86}$-*b*-PGMA$_{82}$	2.26	52.1	1.20	lamella	31.7
P*t*BA$_{86}$-*b*-PGMA$_{40}$	1.67	34.1	1.15	cylinder	26.6
P*t*BA$_{127}$-*b*-PGMA$_{53}$	2.38	31.6	1.11	sphere	31.4

[a] Calculated according to ^{1}H NMR. [b] Determined by GPC with PS standard. [c] Determined by SAXS.

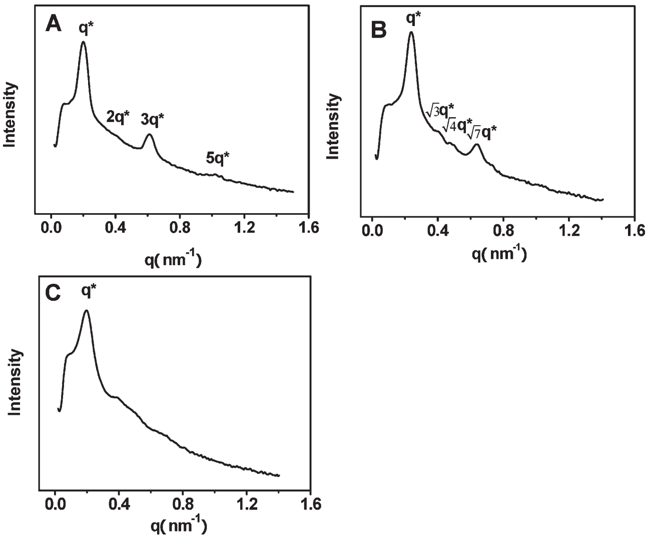

Figure 1. SAXS curves of bulk self-assemblies prepared from (A) P*t*BA$_{86}$-*b*-PGMA$_{82}$, (B) P*t*BA$_{86}$-*b*-PGMA$_{40}$, and (C) P*t*BA$_{127}$-*b*-PGMA$_{53}$.

Bulk Self-Assembly of P*t*BA-*b*-PGMA Diblock Copolymers. The microphase-separated structures of three diblock copolymers with different compositions, P*t*BA$_{86}$-*b*-PGMA$_{82}$, P*t*BA$_{86}$-*b*-PGMA$_{40}$, and P*t*BA$_{127}$-*b*-PGMA$_{53}$, were studied by SAXS, and the results are shown in Figure 1. For the diblock copolymer P*t*BA$_{86}$-*b*-PGMA$_{82}$, whose molecular weight fraction of PGMA block was 52.1%, a highly ordered lamellar morphology was obtained. As shown in Figure 1A, the SAXS curve gave several peaks with a pattern of 1:2:3:5, consistent with a lamellar morphology. From the primary peak position value at low *q*, the average *d*-spacing was calculated to be 31.7 nm. Figure 1B showed the SAXS curve of the self-assembly prepared from P*t*BA$_{86}$-*b*-PGMA$_{40}$ with PGMA weight fraction of 34.1%, and an ordered hexagonally packed cylindrical morphology was obtained. The SAXS curve illustrated a series of peaks with peak position of $1{:}\sqrt{3}{:}\sqrt{4}{:}\sqrt{7}$, consistent with a hexagonally packed cylindrical morphology. From the primary peak position value at low *q*, the average *d*-spacing was calculated to be 26.6 nm. As for the diblock copolymer of P*t*BA$_{127}$-*b*-PGMA$_{53}$ with 31.6% PGMA, the microphase separation produced a liquidlike packing of the spheres with a *d*-spacing of 31.4 nm, as shown in Figure 1C.

The P*t*BA-*b*-PGMA bulk materials contained the epoxy-rich domains as a dispersed phase, which can be cross-linked easily with a variety of amines, either diamine or monoamine. The films with an ordered nanostructure were exposed to the atmosphere of EDA and PA. Since the amines can react with ester bonds as well, the cross-linking reaction time using EDA was limited in 2 h while the reaction time of PA was 4 h. The morphologies of the cross-linked materials were investigated with TEM, and the TEM images of microtomed slices with PA cross-linking are shown in Figure 2. The samples were stained with RuO_4 vapor; therefore, the dark areas in the TEM images were corresponded to the cross-linked PGMA domains. Figure 2A was the TEM photograph of the PA cross-linked P*t*BA$_{86}$-*b*-PGMA$_{82}$, in which an ordered array of alternating P*t*BA and PGMA lamellae was observed. The average *d*-spacing measured from the TEM photograph was 30−31 nm, which was similar to the value obtained from the SAXS curve before cross-linking. Demonstrated in Figure 2B was the corresponding TEM photograph of the cross-linked structure of P*t*BA$_{86}$-*b*-PGMA$_{40}$, in which the arrays of PGMA cylinders perpendicular to the sight were displayed. As revealed in Figure 2C, the TEM image of P*t*BA$_{127}$-*b*-PGMA$_{53}$ microtomed slice displayed a liquidlike packing of cross-linked PGMA spheres as dark particles dispersed in the P*t*BA matrix. The above observation of the cross-linked microphase-separated block copolymers of P*t*BA-*b*-PGMA matched the results of SAXS from the un-cross-linked precursors, demonstrating that the cross-linking process would not destroy the structures of self-assembly of the block copolymers.

Dispersion of Cross-Linked Nanoobjects in Solvent. It is known that the P*t*BAs can be dissolved in variety of organic solvents, and DCM was selected in this section. To prepare dispersed nanoobjects, the cross-linked self-assemblies were immersed in DCM with vigorous stirring. After stirred for 24 h, the bulk materials disappeared and homogeneous dispersions were obtained. As for appearance of the dispersions, the sample of P*t*BA$_{86}$-*b*-PGMA$_{82}$ looked translucent, indicating the large size of dispersion. As for the sample of P*t*BA$_{86}$-*b*-PGMA$_{40}$, the dispersion became transparent, and a blue tint implied the dispersion with small and uniform size. When the sample of P*t*BA$_{127}$-*b*-PGMA$_{53}$ was dispersed, the dispersion became completely clear. The TEM results shown in parts A, B, and C of Figure 3 gave the morphologies of the dispersed nanoobjects with EDA cross-linking prepared from P*t*BA$_{86}$-*b*-PGMA$_{82}$, P*t*BA$_{86}$-*b*-PGMA$_{40}$, and P*t*BA$_{127}$-*b*-PGMA$_{53}$, respectively, and the nanoplates, nanofibers, and nanospheres were well-displayed. As the DCM was a good solvent for both P*t*BA and PGMA blocks, the dispersed nanoobjects indicated that the PGMA domains were cross-linked successfully. As for the PA cross-linked nanoobjects, there were no obvious differences in appearance with the EDA cross-linked ones. This meant that the PA, a monoamine, can also cross-link the PGMA domains. The PA cross-linked nanoobjects prepared from three block copolymers are shown in parts D, E, and F of Figure 3, respectively. As a whole, dispersing the cross-linked lamellar materials of P*t*BA$_{86}$-*b*-PGMA$_{82}$, isolated nanoplates with uniform thickness were obtained by using different amine cross-linkers (Figure 3A,D). Similarly, well-defined nanofibers with a diameter of ca. 27 nm were obtained by dispersing the P*t*BA$_{86}$-*b*-PGMA$_{40}$ (Figure 3B,E), which were inherited from their bulk structures, and the diameters of the fibers were consistent with the *d*-spacing calculated from SAXS. The length of the nanofibers reached several micrometers, and the fibers looked semiflexible. Also, nanospheres (Figure 3C,F) were obtained by dispersing P*t*BA$_{127}$-*b*-PGMA$_{53}$ with a diameter of ca. 35 nm, comparable with the *d*-spacing calculated from SAXS data before cross-linking. These dispersible plates, fibers, and spheres were core−shell structures with the P*t*BA hairs grafted from the cross-linked PGMA cores. Thus, well-defined nanoobjects bearing P*t*BA hairs have been obtained by dispersing the cross-linked self-assemblies in the solvents of the P*t*BA segments (the methanol dispersed nanoobjects are shown in Figure S3 of the Supporting Information). It is of noteworthy that the PA cross-linked nanoobjects had pendant alkyne groups on the cores, which can be applied to anchor functional groups onto the nanoobjects with click reaction[32,33] as shown in the latter section.

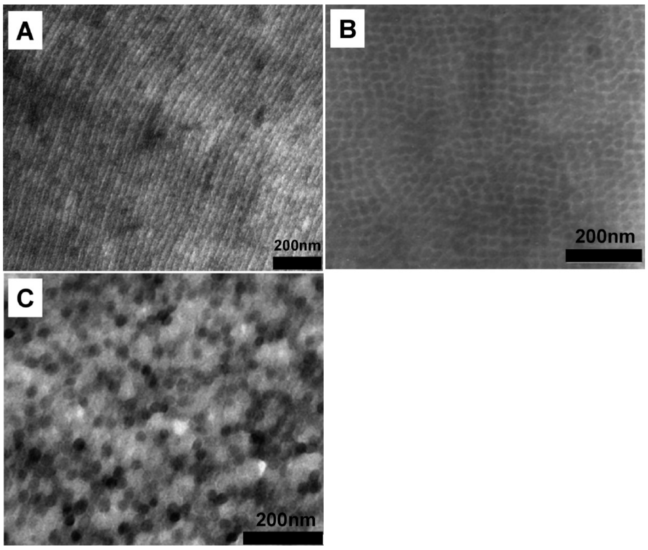

Figure 2. TEM images of microtomed slices of PA cross-linked bulk materials of (A) P*t*BA$_{86}$-*b*-PGMA$_{82}$, (B) P*t*BA$_{86}$-*b*-PGMA$_{40}$, and (C) P*t*BA$_{127}$-*b*-PGMA$_{53}$. The slices were stained by RuO_4.

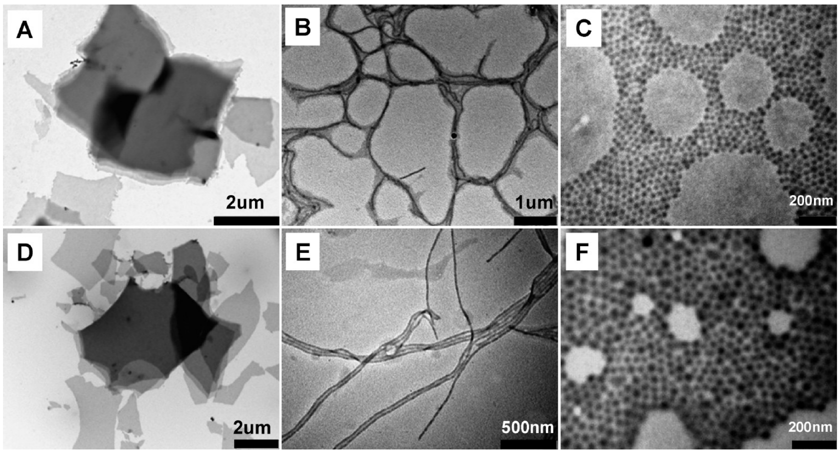

Figure 3. TEM images of the dispersed nanoobjects in DCM with EDA and PA cross-linking. Images A, B, and C were the EDA cross-linked P*t*BA$_{86}$-*b*-PGMA$_{82}$, P*t*BA$_{86}$-*b*-PGMA$_{40}$, and P*t*BA$_{127}$-*b*-PGMA$_{53}$, respectively; images D, E, and F were PA cross-linked ones.

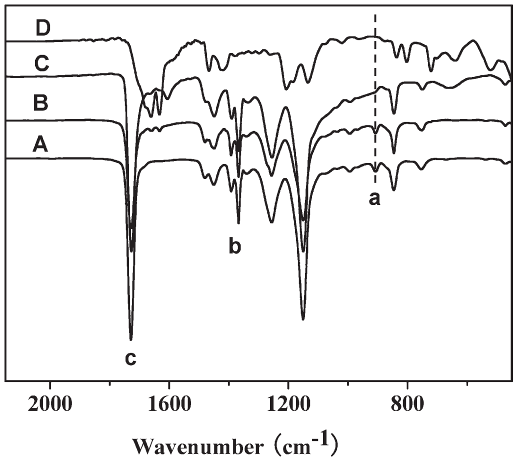

Figure 4. FT-IR spectra of P*t*BA$_{127}$-*b*-PGMA$_{53}$ self-assembly at different stage: (A) before cross-linking; (B) after 2 h EDA cross-linking; (C) after 4 h PA cross-linking; (D) PA cross-linked nanospheres after hydrolysis. Peaks are identified as follows: (a) epoxy stretching (907 cm^{-1}) in PGMA; (b) $-CH_3$ bending (1394, 1368 cm^{-1}) in *t*Bu group; (c) C=O stretching (1730 cm^{-1}) in ester group.

The cross-linking process was traced with FT-IR, and the spectra of P*t*BA$_{127}$-*b*-PGMA$_{53}$ self-assembly at different stages are shown in Figure 4. The absorbance at 907 cm^{-1} in Figure 4A showed the existence of epoxy groups in the P*t*BA-*b*-PGMA self-assembly. The IR spectrum of the EDA cross-linked sample is shown in Figure 4B. Although the morphology was fixed within 2 h of cross-linking reaction, a large amount of epoxy group still existed in the self-assembly (residual absorbance at 907 cm^{-1}). However, the cross-linking reaction was almost completed after the sample was exposed to the PA atmosphere for 4 h (disappearance of 907 cm^{-1} in IR spectrum shown in Figure 4C). It was important that the ester bonds were well-preserved during the cross-linking process (absorbance of C=O at 1730 cm^{-1}). The higher cross-linking extent of PA than that of DEA was mainly due to the different boiling point of cross-linkers (the boiling points of PA and EDA are 84 and 116 °C, respectively) and longer cross-linking time. The remaining epoxys in the DEA cross-linked nanoobjects are very interesting since they could still be applied to introduce different functionalities into these nanoobjects.

To check the remained epoxy, the EDA cross-linked nanoplates from P*t*BA$_{100}$-*b*-PGMA$_{95}$ were treated by NaN_3 in DMF since azide ions react with epoxy quantitatively,[33] as shown in Scheme S1 (in Supporting Information). After purified and dried under vacuum, the FT-IR analysis was performed. Compared with the IR spectrum of the EDA cross-linked nanoplates, the characteristic absorbance of epoxy groups at 907 cm^{-1} disappeared completely, and the characteristic absorbance of azide groups appeared at 2100 cm^{-1},[33] as shown in Figure S4 (in the Supporting Information). This result indicated that the azide groups had introduced into the cross-linked PGMA cores by postmodification of the epoxy groups, implying further modification possibility by Cu(I)-mediated 1,3-dipolar cycloaddition reactions occurred between alkyne and azide.[32,33]

Hydrolysis of P*t*BAs and pH Responsibility of PAA Hairs. Since the P*t*BA hairs were densely tethered from the surfaces of the nanoobjects and were readily to be hydrolyzed into the PAA hairs, the hydrolysis of the nanoobjects cross-linked by PA was explored. Cleavage of the *tert*-butyl (*t*Bu) groups was achieved by treatment of the nanoobjects of three shapes in DCM catalyzed by TFA due to the TFA can remove *t*Bu groups while other ester bonds were well-preserved.[38,39] After 24 h of hydrolysis, the hydrolyzed nanoobjects were extracted with an aqueous solution of KOH, and the water dispersions were dialyzed against water until the pH = 7. The hydrolyzed nanospheres with the PAA hairs were also characterized with FT-IR. As shown in Figure 4C of the spectrum from the sample before treatment with TFA, $-CH_3$ bending at 1394 and 1368 cm^{-1} represented the *t*Bu groups of P*t*BA, and the C=O (ester) stretching at 1730 cm^{-1} ascribed to that of P*t*BA and PGMA. After hydrolyzed for 24 h, the characteristic peaks from *t*Bu groups at 1394 and 1368 cm^{-1} disappeared completely, as shown in Figure 4D. The sharp absorbance of carbonyl groups at 1730 cm^{-1} corresponding to the ester bonds was broadened, and the peak shifted to 1640 cm^{-1} due to the formation of carboxylic ions. This result demonstrated that the *t*Bu groups were removed completely by TFA in 24 h. As shown in Figure 5, the water-dispersed nanoobjects hydrolyzed from the PA cross-linked nanoobjects of P*t*BA$_{86}$-*b*-PGMA$_{82}$, P*t*BA$_{86}$-*b*-PGMA$_{40}$, and P*t*BA$_{127}$-*b*-PGMA$_{53}$ remained as nanoplates (Figure 5A), nanofibers (Figure 5B), and nanospheres (Figure 5C), which indicated that the hydrolysis did not destroy the structures of the nanoobjects. However, it was observed that the diameter of nanofibers decreased from 27 to about 23 nm, while the diameter of nanospheres decreased from 35 to 32 nm. The shrinkage of the diameters was due to the hydrolysis of P*t*BA hairs into PAAs.

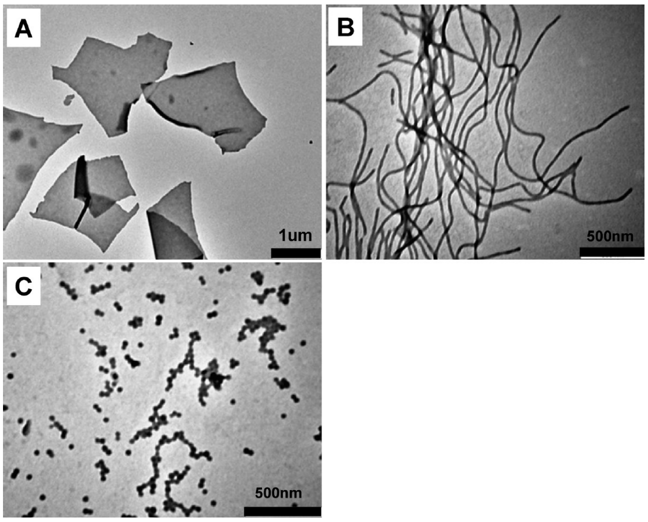

Figure 5. TEM images of water-dispersed nanoobjects hydrolyzed from PA cross-linked (A) P*t*BA$_{86}$-*b*-PGMA$_{82}$, (B) P*t*BA$_{86}$-*b*-PGMA$_{40}$, and (C) P*t*BA$_{127}$-*b*-PGMA$_{53}$.

To examine the pH responsibility of the PAA hairs coated nanoobjects, the pH value of the water dispersions was changed first from pH = 7 to pH = 3 and then to pH = 10. As shown by the optical photographs of the water-dispersed nanoplates in Figure 6A, the as-obtained nanoplates in water dispersion looked translucent. When pH of the dispersion was changed to pH = 3, the nanoplates precipitated to the bottom of the bottle and the upper water became clear (Figure 6B). After the pH was increased to 10, the nanoplates were dispersed again, and the dispersion showed no difference with that of pH = 7, as shown in Figure 6C. Similar results were obtained for the nanofibers and nanospheres (Figures S5 and S6 in the Supporting Information). Moreover the TEM images of the nanoplates after the pH cycle looked no difference with that before the pH cycle (Figure S7 in the Supporting Information). Therefore, the isolated cross-linked nanoobjects densely tethered with PAAs with not only controlled shapes but also pH-responsive characteristics have been obtained by hydrolysis of the

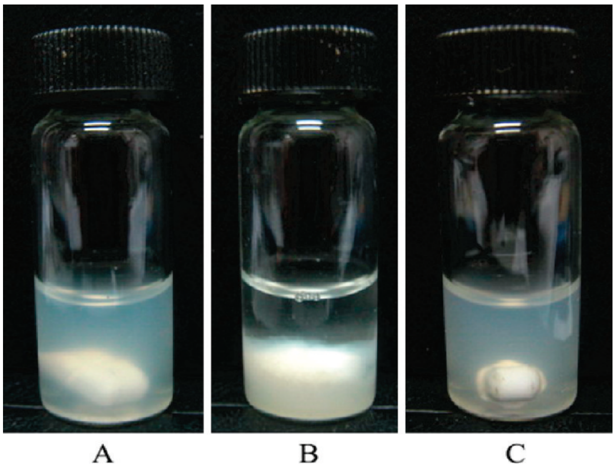

Figure 6. Optical photographs of water-dispersed nanoplates bearing PAA segments at different pH: (A) pH = 7 after dialysis; (B) pH was changed to 3; (C) after pH was titrated to 10.

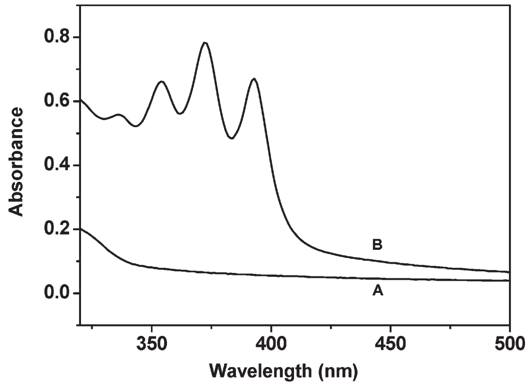

Figure 7. UV spectrum of PA cross-linked nanofibers before (A) and after (B) click reaction with 9-AMA in water dispersion.

Scheme 3. Click Reaction between the PA Core Cross-Linked Nanoobjects and 9-AMA

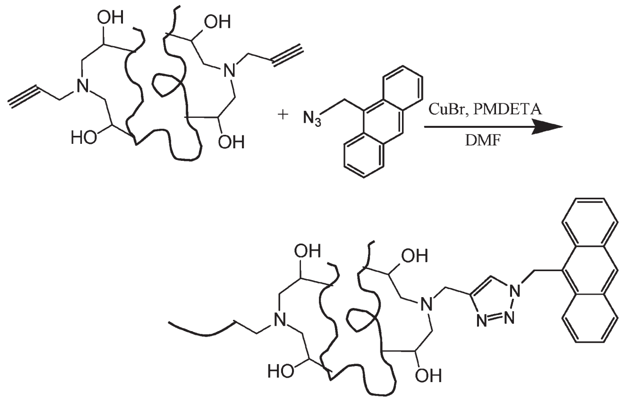

self-assembled P*t*BA-*b*-PGMA diblock copolymers cross-linked by amines.

Click Reaction on PA Cross-Linked Nanofibers. The nanoobjects fixed by PA are very interesting since the alkyne groups have been introduced into the cross-linked cores of these particles simultaneously. Here we have studied postmodification of the PA cross-linked nanofibers by Cu(I)-mediated 1,3-dipolar cycloaddition reaction between the pendant alkyne groups and 9-AMA as a model reaction as shown in Scheme 3. The reaction was carried out between the cross-linked nanofibers of P*t*BA$_{86}$-*b*-PGMA$_{40}$ in DMF dispersion and 9-AMA catalyzed by CuBr/PMDETA. By further removal of *t*BA groups, the nanofibers were extracted into water after washed with DCM thoroughly to remove the unreacted 9-AMA. The UV experiments were performed after the dispersion was dialyzed against water. As shown in Figure 7A, the UV absorption spectrum of the nanofibers without click reaction showed no characteristic absorbance with some scattering in low wavelength region. However, the spectrum of the nanofibers after click reaction (Figure 7B) displayed a characteristic absorbance of anthracene units between $\lambda = 330-400$ nm.[40] This result demonstrated that 9-AMA had been anchored to the nanoobjects by the click reaction, indicating flexible postmodifiable strategy for the present block copolymer nanoobjects of PGMA.

Conclusions

A new class of cross-linkable diblock copolymer P*t*BA-*b*-PGMA was synthesized by ATRP, and the microphase separation of a series of the block copolymers was studied. Since the PGMA segments have been concentrated into the isolated microdomains of different structure, the PGMA domains were facilely cross-linked by exposing the phase-separated materials in an environment of amines. Therefore, this report provided a novel useful platform for fabricating polymeric nanoobjects of functional block copolymers using epoxy chemistry. Its characteristics included (1) the cross-linking chemistry of block copolymer microdomains using epoxy is mild and easy to conduct, (2) functional amines may not only induce the cross-linking but also introduce the functionalities simultaneously, and (3) by mediating the cross-linking ratio, the reaction ratio of epoxy can be changed and the remained epoxy can be used for further introducing other species.

Acknowledgment. Financial support from National Natural Science Foundation of China (50973119, 20534010, and 20625412) is gratefully acknowledged.

Supporting Information Available: SEC traces (Figure S1) of polymerization, ^{1}H NMR spectrum of P*t*BA$_{86}$-*b*-PGMA$_{40}$ (Figure S2), TEM images of methanol dispersed nanoobjects (Figure S3), reaction between epoxy residues and NaN$_3$ and FTIR spectrum (Scheme S1 and Figure S4), pH responsibility of cylinders and spheres (Figures S5−S8), and the properties of different plate formation sample (Figures S9 and S10). This material is available free of charge via the Internet at http://pubs.acs.org.

References and Notes

(1) Bates, F. S.; Fredrickson, G. H. *Annu. Rev. Phys. Chem.* **1990**, *41*, 525–557.
(2) Haryono, A.; Binder, W. H. *Small* **2006**, *2*, 600–611.
(3) Kang, C.; Kim, E.; Baek, H.; Hwang, K.; Kwak, D.; Kang, Y.; Thomas, E. L. *J. Am. Chem. Soc.* **2009**, *131*, 7538–7539.
(4) Ishizu, K.; Fukutomi, T. *J. Polym. Sci., Part C: Polym. Lett.* **1988**, *26*, 281–286.
(5) Hamley, I. W. *Angew. Chem., Int. Ed.* **2003**, *42*, 1692–1712.
(6) Förster, S.; Plantenberg, T. *Angew. Chem., Int. Ed.* **2002**, *41*, 688–714.
(7) Hillmyer, M. A. *Adv. Polym. Sci.* **2005**, *190*, 137–181.
(8) Drockenmuller, E.; Li, L. Y. T.; Ryu, D. Y.; Harth, E.; Russell, T. P.; Kim, H. C.; Hawker, C. J. *J. Polym. Sci., Part A: Polym. Chem.* **2005**, *43*, 1028–1037.
(9) Guo, F. X.; Jankova, K.; Schulte, L.; Vigild, M. E.; Ndoni, S. *Macromolecules* **2008**, *41*, 1486–1493.
(10) Lin, T.; Ho, R. M.; Ho, J. C. *Macromolecules* **2009**, *42*, 742–751.
(11) Gao, L. C.; Yao, J.; Shen, Z. H.; Wu, Y. X.; Chen, X. F.; Fan, X. H.; Zhou, Q. F. *Macromolecules* **2009**, *42*, 1047–1050.

(12) Yan, X. H.; Liu, G. J.; Liu, F. T.; Tang, B. Z.; Peng, H.; Pakhomov, A. B.; Wong, C. Y. *Angew. Chem., Int. Ed.* **2001**, *40*, 3593–3596.
(13) Yan, X. H.; Liu, F. T.; Li, Z.; Liu, G. J. *Macromolecules* **2001**, *34*, 9112–9116.
(14) Yan, X. H.; Liu, G. J.; Li, Z. *J. Am. Chem. Soc.* **2004**, *126*, 10059–10062.
(15) Erhardt, R.; Böker, A.; Zettl, H.; Kaya, H.; Pyckhout-Hintzen, W.; Krausch, G.; Abetz, V.; Müller, A. H. E. *Macromolecules* **2001**, *34*, 1069–1075.
(16) Walther, A.; Drechsler, M.; Müller, A. H. E. *Soft Matter* **2009**, *5*, 385–390.
(17) Yelamanchili, R. S.; Walther, A.; Müller, A. H. E.; Breu, J. *Chem. Commun.* **2008**, *9*, 489–492.
(18) Schacher, F.; Yuan, J. Y.; Schoberth, H. G.; Müller, A. H. E. *Polymer* **2010**, *51*, 2021–2032.
(19) Zhang, K.; Gao, L.; Chen, Y. M. *Macromolecules* **2007**, *40*, 5916–5922.
(20) Zhang, K.; Gao, L.; Chen, Y. M.; Yang, Z. Z. *Chem. Mater.* **2008**, *20*, 23–25.
(21) Zhang, K.; Gao, L.; Chen, Y. M. *Macromolecules* **2008**, *41*, 1800–1807.
(22) Zhang, K.; Gao, L.; Zhang, C.; Chen, Y. M. *J. Mater. Chem.* **2009**, *19*, 3482–3489.
(23) Zhang, K.; Gao, L.; Zhang, C.; Chen, Y. M. *Polymer* **2010**, *51*, 2809–2817.
(24) Cañamero, P. F.; de la Fuente, J. L.; Madruga, E. L.; Fernández-García, M. *Macromol. Chem. Phys.* **2004**, *205*, 2221–2228.
(25) Huang, W.; Zhou, Y. F.; Yan, D. Y. *J. Polym. Sci., Part A: Polym. Chem.* **2005**, *43*, 2038–2047.
(26) Zhu, H.; Liu, Q. C.; Chen, Y. M. *Langmuir* **2007**, *23*, 790–794.
(27) Jiang, X. W.; Xiong, D. A.; An, Y. L.; Zheng, P. W.; Zhang, W. Q.; Shi, L. Q. *J. Polym. Sci., Part A: Polym. Chem.* **2007**, *45*, 2812–2819.
(28) Paul, R.; Karabiyik, U.; Swift, M. C.; Esker, A. R. *Langmuir* **2008**, *24*, 5079–5090.
(29) Connal, L. A.; Li, Q.; Quinn, J. F.; Tjipto, E.; Caruso, F.; Qiao, G. G. *Macromolecules* **2008**, *41*, 2620–2626.
(30) Xu, C.; Wayland, B. B.; Fryd, M.; Winey, K. I.; Composto, R. J. *Macromolecules* **2006**, *39*, 6063–6070.
(31) Nishimura, T.; Ito, T.; Yamamoto, Y.; Yoshio, M.; Kato, T. *Angew. Chem., Int. Ed.* **2008**, *47*, 2800–2803.
(32) Sumerlin, B. S.; Vogt, A. P. *Macromolecules* **2010**, *43*, 1–13.
(33) Meldal, M. *Macromol. Rapid Commun.* **2008**, *29*, 1016–1051.
(34) Lan, P.; Porco, J. A., Jr.; South, M. S.; Parlow, J. J. *J. Comb. Chem.* **2003**, *5*, 660–669.
(35) de la Fuente, J. L.; Cañamero, P. F.; Fernández-García, M. *J. Polym. Sci., Part A: Polym. Chem.* **2006**, *44*, 1807–1816.
(36) Nanjundan, S.; Unnithan, C. S.; Selvamalar, C. S. J.; Penlidis, A. *React. Funct. Polym.* **2005**, *62*, 11–24.
(37) Muñoz-Bonilla, A.; Cerrada, M. L.; Fernández-García, M. *Macromol. Chem. Phys.* **2007**, *208*, 2654–2664.
(38) Bryan, D. B.; Hall, R. F.; Holden, K. G.; Huffman, W. F.; Gleason, J. G. *J. Am. Chem. Soc.* **1977**, *99*, 2353–2355.
(39) Ma, Q.; Wooley, K. L. *J. Polym. Sci., Part A: Polym. Chem.* **2000**, *38*, 4805–4820.
(40) Durmaz, H.; Colakoglu, B.; Tunca, U.; Hizal, G. *J. Polym. Sci., Part A: Polym. Chem.* **2006**, *44*, 1667–1675.